ACS APPLIED MATERIALS & INTERFACES

RESEARCH ARTICLE

www.acsami.org

# New Highly Luminescent Hybrid Materials: Terbium Pyridine−Picolinate Covalently Grafted on Kaolinite

Emerson H. de Faria,*[,†] Eduardo J. Nassar,[†] Katia J. Ciuffi,[†] Miguel A. Vicente,[‡] Raquel Trujillano,[‡] Vicente Rives,[‡] and Paulo S. Calefi*[,†]

[†]Universidade de Franca, Av. Dr. Armando Salles Oliveira, Parque Universitário, 201, 14404-600, Franca, SP, Brazil

[‡]Departamento de Química Inorgánica, Facultad de Ciencias Químicas, Universidad de Salamanca, Plaza de la Merced, S/N, 37008 Salamanca, Spain

Supporting Information

**ABSTRACT:** Luminescent hybrid materials derived from kaolinite appear as promising materials for optical applications due to their specific properties. The spectroscopic behavior of terbium picolinate complexes covalently grafted on kaolinite and the influence of the secondary ligand and thermal treatment on luminescence are reported. The resulting materials were characterized by thermal analysis, element analysis, X-ray diffraction, infrared absorption spectroscopy, and photoluminescence. The thermogravimetric curves indicated an enhancement in the thermal stability up to 300 °C for the lanthanide complexes covalently grafted on kaolinite, with respect to the isolated complexes. The increase in the basal spacing observed by X-ray diffraction confirmed the insertion of the organic ligands into the basal space of kaolinite, involving the formation of a bond between Al−OH and the carboxylate groups, as evidenced by infrared spectroscopy. The luminescent hybrid material exhibited a stronger characteristic emission of $Tb^{3+}$ compared to the isolated complex. The excitation spectra displayed a broad band at 277 nm, assigned to a ligand-to-metal charge transfer, while the emission spectra presented bands related to the electronic transitions characteristic of the $Tb^{3+}$ ion from the excited state $^5D_4$ to the states $^7F_J$ ($J$ = 5, 4, and 3), with the 4→5 transition having high intensity with green emission.

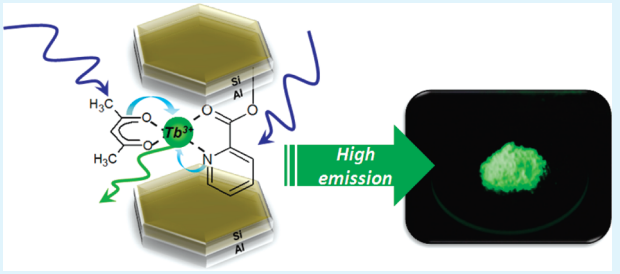


**KEYWORDS:** kaolinite, functionalization, hybrid materials, terbium complexes, picolinate, photophysical properties

## 1. INTRODUCTION

The spectroscopic properties of complexes formed between lanthanide ions and organic ligands allow for a wide range of applications, including luminescent sensors, lasers, optic fibers, amplifiers, and electroluminescent materials.[1−3] In these materials, the organic ligands intensify the energy absorption (antenna effect), but the isolated complexes present low thermal and chemical stability, indicating the need to support them onto inorganic matrixes.[4−7]

In this context, the unique properties and functionality of hybrid materials obtained by modification of the surface of clay minerals have attracted growing attention from scientists worldwide. Recently, inorganic matrixes such as zeolites, silica, titania, alumina, and natural or synthetic clays, e.g., kaolinite, montmorillonite, hectorite, laponite, and saponite, have been combined with organic compounds like aminoalcohols, polyalcohols, polymers, alkoxides, pyridine−carboxylic acids, porphyrins, and others for the development of organic−inorganic hybrids, composites, and nanocomposites.[8−16]

Layered matrixes can be modified by intercalation and/or functionalization of organic molecule, or anion, ligands, thereby producing hybrid organic−inorganic materials with specific properties, which in turn depend on the interaction, covalent bond in functionalization, and intermolecular forces in intercalated compounds. In this context, some smectite group layered clay materials (bentonites) with 2:1 (or TOT, tetrahedra−octahedra−tetrahedra) structure and layered double hydroxides have been modified with luminescent complexes such as Tb(bipy)$_2$(NO$_3$)$_3$, Tb(bipy)$_2$Cl$_3$(H$_2$O), Eu(bipy)$_2$Cl$_3$, and Eu(phen)$_2$.[17−21] Several studies have been conducted with these groups of clay minerals, because of their easy expansion and high cation exchange capacity. In general, the majority of papers devoted to luminescence have used complexes of Eu(III) or Tm(III) incorporated to different matrixes. Although much less studied, Tb(III) has singular spectral properties, due to very sharp emission bands (sharper than usual luminescent organic molecules) and high green emission produced only by 4f−4f rare earth emissions.

On the other hand, kaolin is a clay mineral very abundant worldwide. It is mainly composed of kaolinite, which presents the theoretical formula $Al_2Si_2O_5(OH)_4$, with a basal interlayer space of 7.14 Å and 1:1, or TO, tetrahedra−octahedra, structure; i.e., it is a dioctahedral aluminosilicate layered clay. Two kinds of interlayer surfaces are found in this mineral clay, namely, [SiO$_6$] macro-rings

Received: January 26, 2011
Accepted: March 29, 2011
Published: March 29, 2011

  

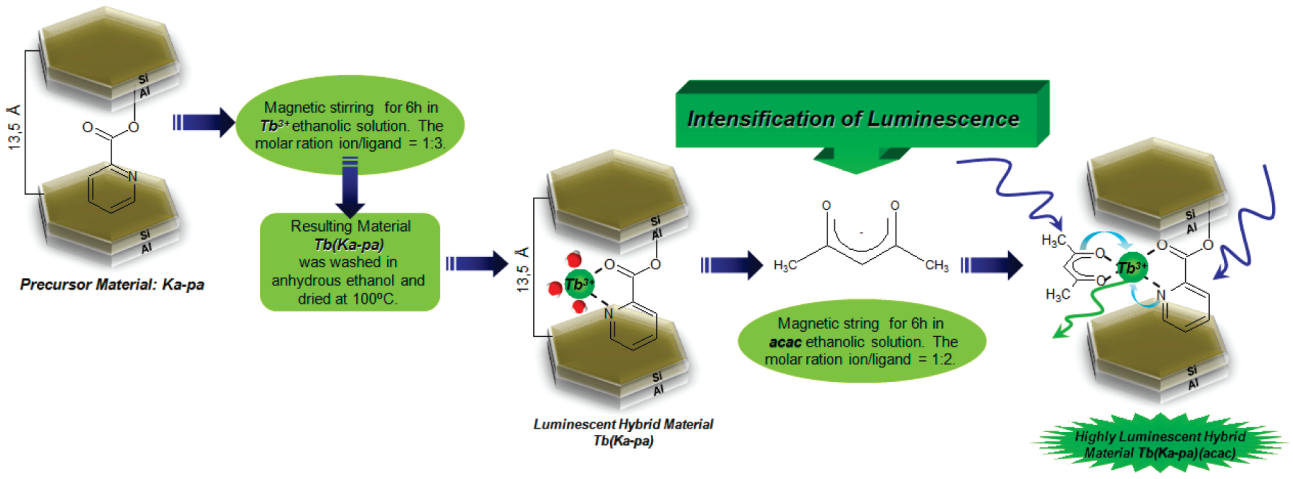


**Figure 1.** Scheme of the procedure employed for the preparation of luminescent hybrid materials based on kaolinite.

on one side and gibbsite aluminol groups [$Al(OH)_3$] on the other side, giving rise to lamellas. The presence of hydroxyl groups in the interlayer space of kaolinite allows for their covalent modification by condensation reactions.[13,22−29]

The uses of the TOT clays, such as saponite and montmorillonite, modified with luminescent complexes are limited because the weak interactions between the organic compound and the clay promote low chemical and thermal stability, so the organic species can be easily leached from these matrixes. Another fact that limits the use of clays with TOT structure is the presence of water molecules coordinated to the cations in their interlayer space. The water molecules promote quenching of the luminescence of the lanthanide by nonradiative decays from excited to fundamental states.[30,31] Thus, although the intercalation of kaolinite is more difficult, the immobilization of complexes into its interlayer region may be much more effective.

Some organic ligands intensify the energy absorption in lanthanide cations (antenna effect), but the isolated complexes have low thermal stability, which reduces the technological applications of these compounds. Supporting lanthanide complexes on inorganic matrixes such as silica, alumina, zeolites, and clays is one of the possibilities for avoiding this inconvenience.[32] One class of organic ligands that has attracted a lot of attention from countless researchers is that of pyridine carboxylic and dicarboxylic acids including nicotinic, isonicotinic, quinolinic, picolinic, and dipicolinic acids. These ligands are commonly used in the formation of different complexes with a large variety of transition metals (see Figure S1, Supporting Information).[33−35] These ligands show large absorption spectra that can promote the charge transfer with Tb(III) ions by "antenna effect". The efficiency of picolinic acid derivatives as sensitizers is better than that of salicylate derivatives, 1,10-phenanthroline derivatives and $\beta$-diketones due to their efficient "antenna effect".

In this context, the present paper discusses the functionalization of the Brazilian São Simão's kaolinite with a terbium(III) picolinate complex. The effects of the thermal treatment and the incorporation of a secondary ligand on the luminescence of the lanthanide ion are also described. Structural and spectroscopic properties have been evaluated by thermal and chemical analyses, X-ray diffraction, and infrared absorption and luminescence spectroscopies. These materials may potentially be used as sensory probes, in lighting applications (light-emitting diode, LEDs, and flexible organic light-emitting device, FOLEDs), and in lasers. $Tb^{3+}$ green emissions can also monitor as a function of UV/excitation/exposure time, giving a rise to dosimetric sensitivity control.

## 2. EXPERIMENTAL SECTION

**2.1. Sample Preparation.** *a. Incorporation of Terbium on Kaolinite−Picolinate Hybrid Material.* Initially, terbium oxide ($Tb_4O_7$, Aldrich, 99.99%) was heated at 900 °C for 2 h. The calcined oxide was slowly dissolved on 6 mol $L^{-1}$ hydrochloric acid, at 60 °C. The excess of the acid was eliminated by successive addition of water, followed by evaporation, a process repeated by several times. Finally, the amount of water was adjusted for having a $Tb^{3+}$ concentration of 0.10 mol $L^{-1}$.

The kaolin used in this work came from the municipality of São Simão in the State of São Paulo, Brazil, and was kindly supplied by the mining company Darcy R. O. Silva and Cia. The separation of the <2 $\mu$m size particles led to a fraction composed almost exclusively by kaolinite. Between the pyridine−carboxylic acids, picolinic acid was selected for this work (IUPAC name: pyridine−2-carboxylic acid; see its structure in Figure S1, Supporting Information), and kaolinite was grafted by soft-guest methodology with picolinate anions according to the methodology described by de Faria et al.[13] The solid obtained being called Ka-pa. The luminescent hybrid material was prepared by suspending a given amount of Ka-pa in a 0.1 mol/L $Tb^{3+}$ ethanolic solution at a cation/ligand molar ratio of 1:3. The mixture was stirred for 3 h; then, the suspension was centrifuged, and the solid was washed with ethanol five times and dried overnight at 80 °C. The resulting material was designated Tb(Ka-pa).

*b. Incorporation of the Secondary Ligand (Coligand).* Acetylacetonate (acac) was used as secondary ligand. The solid Tb(Ka-pa) was stirred for 6 h in a sodium acetylacetonate ethanolic solution at a $Tb^{3+}$/acac molar ratio of 1:2. The resulting material was washed five times with ethanol and dried overnight at 80 °C. The resulting sample was labeled as Tb(Ka-pa)(acac). The scheme presented in Figure 1 summarizes the procedure involved in the preparation of the luminescent hybrid materials.

**2.2. Influence of Temperature.** On the basis of thermal analysis of sample Tb(Ka-pa) (see Figures 4 and S2, Supporting Information), the luminescent hybrid material was heat-treated for 2 h at 200, 300, or 400 °C. The resulting materials were designated as Tb(Ka-pa)-200, Tb(Ka-pa)-300, and Tb(Ka-pa)-400, respectively.

**2.3. Characterization Techniques.** The amount of $Tb^{3+}$ ion incorporated into the kaolinite hybrid matrix was quantified by the

arsenazo(III) method, according to Marczenko.[36] This spectrophotometric method is sensitive for the quantitative determination of rare earth ions. To this end, the samples were treated with concentrated hydrochloric acid; the remaining solids were heated for 3 h at 50 °C and removed by filtration. The resulting solution was transferred to round-flat bottom flasks of 25 mL, and the volume was completed with distilled water.

The powder X-ray diffractograms of the solids were acquired on a Siemens D-500 diffractometer operating at 40 kV and 30 mA (1200 W), using filtered Cu Kα radiation and varying the $2\theta$ angle from 2° to 65°. All the analyses were processed at a scan speed of 2° ($2\theta$) per minute.

Infrared absorption spectra were obtained on a Perkin-Elmer 1739 spectrometer with Fourier transform, using the KBr pellet technique. Thermal analyses (thermogravimetry (TG)/differential scanning calorimetry (DSC)) were carried out in a TA Instruments SDT Q600 Simultaneous differential thermal analysis (DTA)−thermogravimetric analysis (TGA) thermal analyzer, in the temperature range of 25−1100 °C, at a heating rate of 20 °C/min, and under an air flow of 100 mL/min. The C and N element chemical analysis of the functionalized materials was conducted on a Perkin-Elmer CHN 2400 analyzer.

The emission and excitation spectra were recorded at room temperature on a Jobin Yvon SPEX TRIAX 550 FLUOROLOG III spectrofluorometer. Using the apparatus software, all the spectra were corrected for the lamp intensity and for the sensitivity of the photomultiplier at the monitored wavelength ranges. The luminescence lifetime measurements were achieved using a SPEX 1934D phosphorimeter, equipped with a pulsed xenon lamp. With the aim at minimizing instrumental influences, all the emission, excitation, and lifetime measurements were carried out using a filter with absorption below 450 nm at the exit (detection) of the light beam. The emission spectra were registered with 0.2 nm emission bandpass; excitation spectra and decay curves were obtained with 1 nm emission bandpass. The values of integrated emission intensities and the exponential decay fittings for lifetimes were calculated according to the equation $\tau^{-1} = A_r + A_{nr}$, where $A_r$ is the radiative decay and $A_{nr}$ is the nonradiative decay, and the adjusted curves were obtained from Microcal Origin 6.0 software by the equation $y = A_1 e^{-(x/t_1)} + A_2 e^{-(x/t_2)} + y_0$.

## 3. RESULTS AND DISCUSSION

The X-ray diffractograms of the precursor Ka-pa and of the samples Tb(Ka-pa) and (acac)Tb(Ka-pa) are given in Figure 2. Treatment of kaolinite with picolinic acid produced an increase in the basal distance of the clay, from 7.2 Å in pure kaolinite to 13.5 Å in Ka-pa solid. This clearly shows that the acid molecules were inserted into the interlayer region of the clay; only a few layers of kaolinite (14%) were not intercalated, maintaining the peak at 7.2 Å.[13] Insertion of $Tb^{3+}$ ion into Ka-pa did not provoke any further variation in the basal distance. It may be remarked that the pH was not externally controlled during the process; in each moment, it attained the value produced by the own reagents, and as the p$K_a$ of the carboxylic−carboxylate equilibrium is 5.32, both species can occur in the different stages of the synthesis. The strong chelating ability of picolinate anions and its strong affinity by $Tb^{3+}$ cations may move this equilibrium to the formation of the anion. The substitution of dimethylsulfoxide (DMSO) by picolinic acid in the interlayer region of the DMSO precursor was very effective; 85% of the layers were intercalated by picolinic acid. However, the insertion of $Tb^{3+}$ provoked the removal of some pa molecules; the number of intercalated layers decreased to 67%, and the same happened during the treatment with acac. The final solid had 49% of intercalated layers. As the entrance of $Tb^{3+}$ to the interlayer region is difficult, the strong affinity of the cation for the picolinate anions probably makes

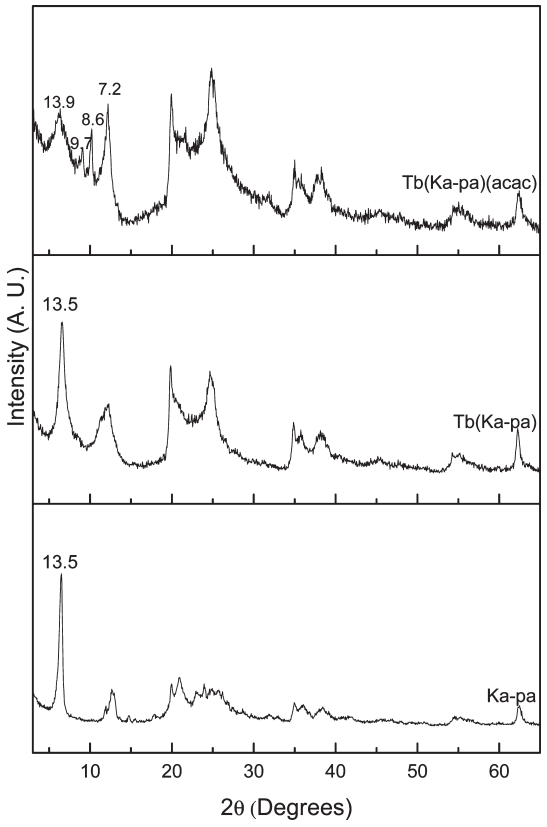


**Figure 2.** XRD powder diffraction patterns ($2\theta = 2-65°$) of kaolinite grafted with picolinate (Ka-pa) and its derivatives Tb(Ka-pa) and Tb(Ka-pa)(acac).

them to go out of the interlayer region, forming soluble Tb-pa complexes removed during the centrifugation and washing.

This also explains the strong decrease of the amount of C and N observed during this treatment (vide infra). However, in the specific case of the sample Tb(Ka-pa)(acac), insertion of the secondary ligand into the interlayer region of kaolinite resulted in a slight increase of the basal distance (13.9 Å). At the same time, other phases with smaller basal distances of 8.6 Å and 9.7 Å were observed. These basal spacings may correspond to kaolinite intercalated with acac or with pa and acac adopting different orientations, but it may also be taken into account that the treatment of kaolinite with certain organic molecules can lead to the formation of tubular kaolinite phases, whose basal spacings have been reported in this range.[37−40] At the same time, a significant amorphization of the solid becomes evident, since the peaks were broader and less intense than before the treatment.

Structurally, kaolinite is characterized by aggregates of TO layers, which consist of one sheet of tetrahedral $SiO_4$ and another sheet of octahedral $Al(OH)_6$. These layers interact by formation of hydrogen bonds between SiO and HO-Al. Insertion of picolinate anions reduces the interlayer cohesive force that maintains the structure of kaolinite. Addition of a secondary ligand (acac) promotes the curling of the kaolinite layers because of the decreased interaction between them. The curling process is known to be favored when the hydrogen bonds of the kaolinite structure are weakened by intercalation or grafting of polar molecules. Indeed, Gardolinsky et al. have attributed the curling of kaolinite layers to the intercalation of large molecules, such as *n*-alkylamine and octadecylamine. This justifies the formation

of distinct phases after insertion of acac.[37−40] The basal interlayer spaces of the kaolinite hybrid materials are summarized in Table 1.

**Table 1. Basal Interplanar Space, $d_{001}$, Variation of the Interplanar Space ($\Delta d$), and Intercalation Ratio ($\alpha$) of the Luminescent Hybrid Materials in Relation to Purified Kaolinite**

| sample | $d_{001}$ (Å) | $\Delta d$ (Å) | $\alpha^a$ (%) |
|---|---|---|---|
| Ka | 7.14 | | |
| Ka-pa | 13.50 | 6.36 | 85 |
| Tb(Ka-pa) | 13.50 | 6.36 | 67 |
| Tb(Ka-pa)(acac) | 13.90 | 6.76 | 49 |

[a] The intercalation ratio ($\alpha$) was quantified according to the relative intensities of the $d_{001}$ peaks in relation to the peak of purified kaolinite. $\alpha = I/(I + I_0)$, $I$ = intensity of the 001 reflection of the product, $I_0$ = intensity of the 001 reflection of unreacted kaolinite.

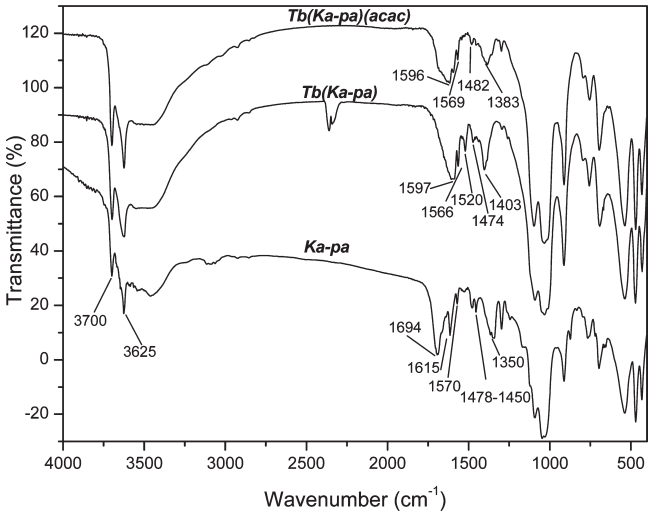


**Figure 3.** Infrared absorption spectra of kaolinite grafted with picolinic acid (Ka-pa) and its derivatives Tb(Ka-pa) and Tb(Ka-pa)(acac).

The infrared absorption spectra of the hybrid materials Ka-pa, Tb(Ka-pa), and displayed Tb(Ka-pa)(acac) (Figure 3) bands at 3625 and 3660 $cm^{-1}$, assigned to the so-called inner and inner surface hydroxyl groups, respectively.[13,22−29] New bands of free hydroxyl groups were not observed after incorporation of the $Tb^{3+}$ ions, although an important amount of picolinic acid is removed during this treatment; it became evident that the molecules actually bonded to the hydroxyl groups forming the hybrid were not modified by the incorporation of the $Tb^{3+}$. The antisymmetric and symmetric stretching vibrations of the carboxylate group incorporated were observed at 1689, 1570, and 1478 $cm^{-1}$ ($COO^-_{asym}$) and 1350 $cm^{-1}$ ($COO^-_{sym}$).[13] After incorporation of the $Tb^{3+}$, these peaks shifted to 1597, 1566, and 1521 $cm^{-1}$ ($COO^-_{asym}$) and 1403 $cm^{-1}$ ($COO^-_{sym}$), respectively. This shifting clearly suggests an interaction between the lanthanide ion and the carboxylate anions present in the hybrid matrix. Further peak shifts were noticed after incorporation of the secondary ligand; Tb(Ka-pa)(acac) exhibited peaks at 1596, 1568, and 1383 $cm^{-1}$; the presence of acac slightly modifies the interaction between the picolinate anions grafted into kaolinite and $Tb^{3+}$. All the infrared (IR) assignments are summarized in Table 2.

Thermal analysis of the precursor Ka-pa and of the samples Tb(Ka-pa) and (acac)Tb(Ka-pa) are depicted in Figures 4 and S2, Supporting Information. The curves of Ka-pa solid show a small mass loss at 75 °C, corresponding to the loss of water molecules adsorbed onto the kaolinite matrix. The decomposition of picolinate is centered at 370 °C, while the small effect due to dehydroxylation is centered at 470 °C.[13,22−29] The exothermic peak at 1000 °C is ascribed to the mullite nucleation.

After incorporation of the $Tb^{3+}$ ion, the curves change considerably, particularly with respect to the peaks related to the decomposition of the organic phase. The percentage of water and solvent molecules in the samples are higher for both Tb(Ka-pa) and (acac)Tb(Ka-pa) compared with Ka-pa, leading to mass losses of about 5% below 100 °C. The organic ligands decompose in three steps at maximum temperatures of 230, 375, and 465 °C in the case of the Tb(Ka-pa) sample and of 245, 379 (shoulder), and 455 °C in the case of the Tb(Ka-pa)(acac) sample. The mass loss with maximum centered at 245 °C, lower than in Ka-pa solid (375 °C),

**Table 2. Assignments of the Infrared Absorption Bands of Ka-pa and its Luminescent Hybrid Derivatives Tb(Ka-pa) and (acac)Tb(Ka-pa)**

| | Ka-pa ($cm^{-1}$) | Tb(Ka-pa) ($cm^{-1}$) | Tb(Ka-pa)(acac) ($cm^{-1}$) |
|---|---|---|---|
| $\nu$ $(OH)_{inner}$ | 3625 | 3625 | 3625 |
| $\nu$ $(OH)_{inner\ surface}$ | 3700 | 3700 | 3700 |
| Si−O | 1025, 1046, 1091 | 1025, 1046, 1091 | 1025, 1046, 1091 |
| $\nu$ Al−$OH_{inner}$ | 912 | 912 | 912 |
| $\nu$ Al−$OH_{inner\ surface}$ | | | |
| $SiO_2$ or quartz | 795 | 795 | 795 |
| $\delta$ Si−O−Al | 760 | 760 | 760 |
| $\delta$ Si−O−$Si_{out\ of\ plane}$ | 698 | 698 | 698 |
| $\delta$ Si−O−$Al_{oct}$ | 536 | 536 | 536 |
| $\delta$ Si−O−$Si_{in\ plane}$ | 467 | 467 | 467 |
| Si−O | 432 | 432 | 432 |
| $\nu_{ass}$ COO | 1700, 1570, 1456 | 1597, 1566 1521 | 1596, 1568 |
| $\nu_{sym}$ COO | 1350 | 1403 | 1383 |
| $\nu$ C=C or C=$N_{(aro)}$ | 1615 | 1566 | 1595 |
| $\beta$ C−H | 1295, 1161, 1117, 1090 | 1295, 1161, 1117, 1090 | 1295, 1161, 1117, 1090 |

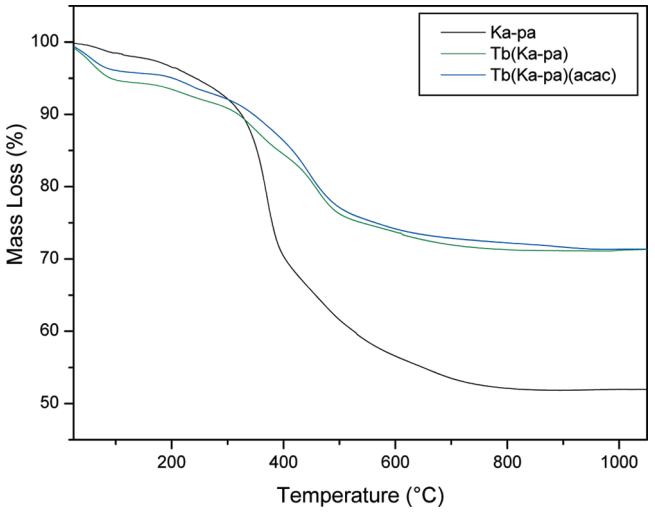


**Figure 4.** TG curves of Ka-pa, Tb(Ka-pa), and Tb(Ka-pa)(acac) performed in $O_2$ atmosphere.

is explained by the leaching of picolinate anions promoted by the insertion of $Tb^{3+}$ cations, confirming the presence of free ligands and isolated complexes adsorbed on surface of the clay, with lower thermal stability than those grafted on kaolinite layers. Bearing in mind that the mass loss around 370 °C in the TG analysis of Ka-pa is undoubtedly due to the loss of picolinate, the peaks at 375 and 379 °C observed for the Tb(Ka-pa) and Tb(Ka-pa)(acac) samples also can reasonably be assigned to this species, not coordinated to the lanthanide. Thus, the peaks at higher temperatures seem to be due to the picolinate anions coordinated to $Tb^{3+}$, their decomposition being observed at 465 and 455 °C, for Tb(Ka-pa) and (acac)Tb(Ka-pa), respectively. In the case of Tb(Ka-pa)(acac), the decomposition of acac ligands seems to be masked by the wide effect due to picolinate. In the high temperature region, after 800 °C, the obtained solids consist of a mixture of $Al_2O_3$, $SiO_2$, and $Tb_4O_7$.[13,22−29]

The elemental analysis of the solids (Table 3) shows that the C/N ratio in the picolinic acid functionalized solid, 4.83, is very close to that in the picolinic acid molecule (5.14). This ratio slightly increases to 6.12, with the incorporation of $Tb^{3+}$, which may be due to the retention of small amounts of ethanol used as solvent in the incorporation of this cation. As it may be expected, this value considerably increases, to 8.99, after the incorporation of secondary ligand acac; this ligand contains C but not N in its structure. This increase clearly suggests the substitution of water molecules by acac ligand (see below discussion of photoluminescence data). Considering the employed pa/Tb = 3 ratio and that pa is a bidentate ligand, pa may coordinate up to six positions for each Tb, but such a coordination may be geometrically difficult to reach in the restricted interlayer region of the clay. However, even if this occurs, the coordination of terbium will be not complete, as its preferred coordination number is usually 7−9. All this justifies the incorporation of acac as a secondary ligand. Considering the amount of N in the Tb(Ka-pa)(acac) solid, the amount of pa molecules can be easily calculated (assuming the theoretical ratio C/N in pa), and from it the amount of acac molecules, leading to a ratio of pa/acac = 1.005.

The amount of pa is clearly lower in Tb(Ka-pa) sample than in the precursor Ka-pa. As suggested before, it seems that pa molecules intercalated in the interlayer but not effectively grafted

**Table 3. C and N Chemical Analysis of Picolinic Acid-Containing Solids and Structural Formulas of the Resulting Complexes**

| structural formula | C content (%) | N content (%) | C/N molar ratio | Tb (mol/g) |
|---|---|---|---|---|
| Ka-$(pa)_{1.59}$ | 25.0 | 5.18 | 4.83 | |
| TbKa-$(pa)_{2.10}$ | 8.64 | 1.41 | 6.12 | $4.77 \times 10^{-4}$ |
| TbKa-$(pa)_{1.20}(acac)_{1.19}$ | 7.52 | 0.80 | 9.40 | $4.74 \times 10^{-4}$ |

to the layers are removed during the incorporation of Tb. This may also be favored by the use of an ethanolic solution in the incorporation of Tb. The treatment with the secondary ligand induces a further removal of intercalated pa molecules, substituted by the acac ones; the removal of water may do that they also participate in the coordination of $Tb^{3+}$. The amount of pa was calculated from the content of N in the solids, and in the case of Tb(Ka-pa)(acac) solid, the amount of C corresponding to pa was calculated; the rest of C might correspond to acac molecules. This allows calculating the following formulas: $Tb(pa)_{2.10}$ in Tb(Ka-pa) sample and $Tb(pa)_{1.20}(acac)_{1.19}$ in Tb(pa)(acac) solid. Thus, the coordination due to the organic ligands clearly increases with the incorporation of the secondary ligand, from 4.20 to 4.78 positions (considering the bidentate character of both ligands), but some coordination positions may still be occupied by water molecules or surface hydroxyl groups. In spite of the strong affinity of both chelating ligands by $Tb^{3+}$, the steric constraints inside the kaolinite layers probably avoid the coordination of the cations to be completed by these ligands.

The luminescence spectra of the terbium−kaolinite solids, registered at room temperature, are shown in Figure 7. All the main features of the excitation spectrum of the free complex are also found in the grafted one.[33,41] The excitation spectrum of the Tb(Ka-pa) sample monitored at 545 nm has two bands, with maxima centered at 275 and 310 nm (Figure 7). These maxima are distinct from those of the free $Tb^{3+}$ cation in aqueous solution (368 nm) and of the free ligand (197, 217, and 265 nm, see Supporting Information). The band at 275 nm can thus be assigned to ligand-to-metal charge transfer (LMCT).[33,41,42] It is evident that an interaction occurs between the lanthanide ion and the ligand, which proves that the picolinic acid grafted on kaolinite absorbs the excitation energy and transfers it to the $Tb^{3+}$ ions efficiently.

After incorporation of the secondary ligand, the excitation maxima centered at 275 and 310 nm shift to 283 and 318 nm, respectively (Figure 5), confirming the substitution of water molecules by the acac ligand, already indicated by the thermal and elemental analyses. The displacement of the band relative to LMCT from 275 to 283 nm can be due to the formation of the new terbium complex with the picolinic acid and acac ligands.

Figure 6 shows the emission spectra of the terbium complexes grafted on kaolinite. The characteristic emission spectrum of the $Tb^{3+}$ ion displays bands at 545, 631, and 670 nm, assigned to transitions from the $^5D_4$ to the $^7F_J$ level ($J$ = 5, 4, and 3), respectively. After incorporation of acac, the appearance of three Stark components can be noticed for the $^5D_4 \rightarrow {}^7F_5$ transition (at about 545 nm), not to mention that the other bands become sharper and more intense. This is evidence that the nonradiative decays promoted by water molecules are reduced or totally eliminated after incorporation of the secondary ligand. No emission bands relative to the free ligands can be observed. This

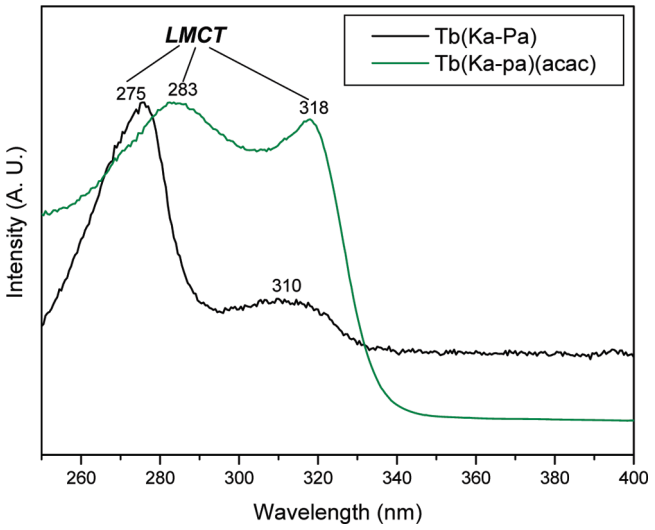


**Figure 5.** Room temperature excitation spectra of the samples Tb(Ka-pa) and Tb(Ka-pa)(acac).

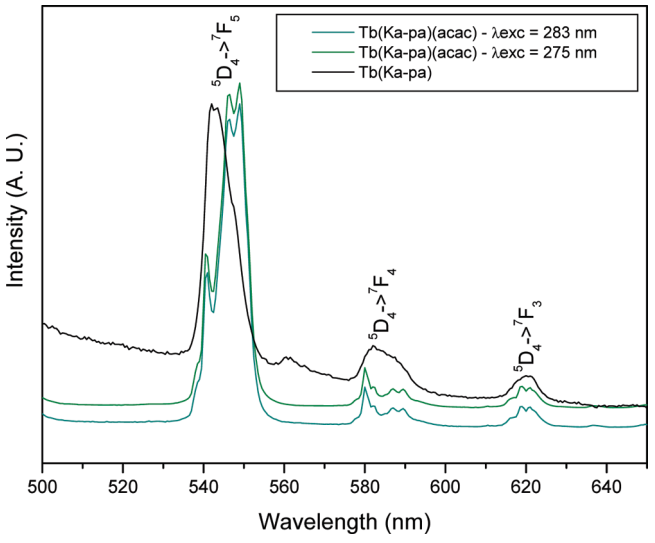


**Figure 6.** Room temperature emission spectra of the samples Tb(Ka-pa) and Tb(Ka-pa)(acac).

indicates that, as picolinic acid, the acac ligand absorbs the excitation energy and transfers it to the chelated $Tb^{3+}$ ions efficiently. Table 4 shows that the $^5D_4 \rightarrow {}^7F_J$ transitions ($J = 5-3$) are split into their respective maximum number of $(2J + 1)$ components.

The luminescence decay of the terbium complexes grafted into kaolinite was measured under excitation at 275 and 310 nm, and a biexponential function with lifetimes of 0.163 and 0.638 ms, respectively, were obtained for the $^5D_4$ state, using ORIGIN software (see Figures S4, S5, and S6 in Supporting Information). The monoexponential decay suggests the existence of one type of site or two types of sites with a very similar environment for each cation complex. On the basis of lifetime values, the number of coordinated water molecules was determined according to the methodology reported by Supkowski and Horrocks Jr.[43] The Tb(Ka-pa) sample has a site with a low amount of water

**Table 4. Lifetime Values for Terbium Complexes Grafted on Kaolinite under Different Wavelength of Excitation**

| sample | $\lambda_{exc}$ (nm) | $\tau_1$ (ms) (%)[a] | $\tau_2$ (ms)( %)[a] |
|---|---|---|---|
| Tb(Ka-pa) | 275 | 0.163 (85) ± 0.004 | 0.638 (15) ± 0.007 |
| Tb(Ka-pa)(acac) | 283 | 1.562 (100) ± 0.005 | |
| Tb(Ka-pa)(acac) | 315 | 1.634 (100) ± 0.010 | |
| Tb(Ka-pa)-200 | 275 | 0.182 (54) ± 0.004 | 0.677 (45) ± 0.008 |
| Tb(Ka-pa)-300 | 275 | 0.126 (61) ± 0.003 | 0.554 (39) ± 0.009 |
| Tb(Ka-pa)-400 | 275 | 0.125 (72) ± 0.004 | 0.535 (28) ± 0.018 |

[a] In parentheses, the percentage of contribution of each site to the luminescence of $Tb^{3+}$ ions.

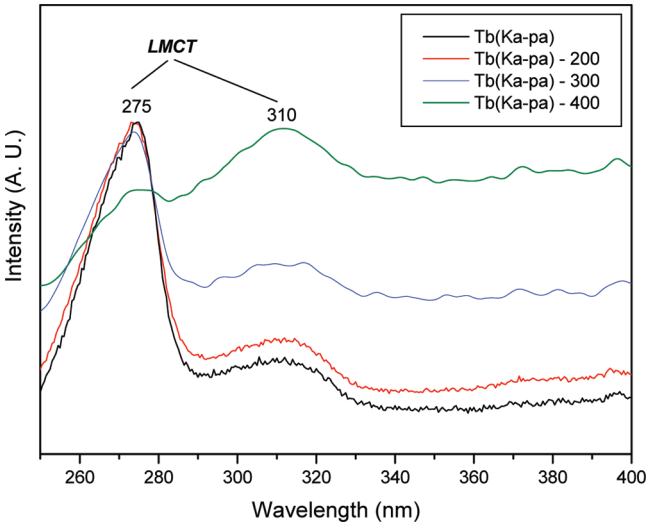


**Figure 7.** Room temperature excitation spectra of the samples Tb(Ka-pa) and the samples heated-treated at 200, 300, and 400 °C.

molecules and another site with a large quantity of coordinated water. The different coordination environment clearly suggests that $Tb^{3+}$ cations occupy two different positions in the kaolinite matrix; it can be reasonably proposed that one of them correspond to $Tb^{3+}$ coordinated to picolinic acid molecules grafted on the clay matrix and in the other the main ligands of $Tb^{3+}$ are the free hydroxyl groups and water molecules present in the interlayer space of kaolinite.

After insertion of the secondary ligand, the water molecules coordinated to the lanthanide ions are totally substituted, and the acac ligand effectively increases the luminescence and lifetime in Tb(Ka-pa)(acac) sample. The lifetimes of 1.562 and 1.634 ms under excitation at 283 and 315 nm, respectively, evidence the absence of water molecules in the surroundings of the $Tb^{3+}$ cation in this solid. Our results also prove the effective participation of the acac ligand in the absorption−transfer−emission process. The isolated complex $Tb(acac)_3$ presents a lifetime of 0.5846 ms, according to Yan and Zhou.[44] The high efficiency in terms of lifetime achieved for the hybrid Tb(Ka-pa)(acac) can be explained by the effective substitution of all the water molecules present in interlayer space of the clay mineral and to the rigid structure of the material, which reduced the energy loss by mechanical vibration modes. The relaxation time of the hybrid materials covalently bound to kaolinite in the excited state becomes long in contrast with those of pure complexes, as

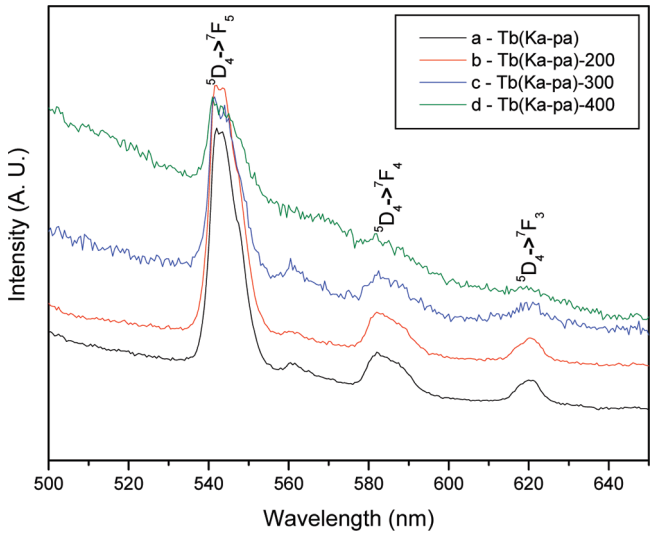


**Figure 8.** Room temperature emission spectra of the samples Tb(Ka-pa) and the samples heated-treated at 200, 300, and 400 °C.

**Table 5. Stark Levels Corresponding to the $^5D_4 \rightarrow {}^7F_J$ ($J$ = 5, 4 and 3) Transition Observed in the Emission Spectra of the Luminescent Hybrid Materials**

| sample | transition | energy ($cm^{-1}$) | wavelength (nm) |
|---|---|---|---|
| Tb(Ka-pa) | $^5D_4 \rightarrow {}^7F_5$ | 18450 | 542 |
| | | 18382 | 544 |
| | | 17857 | 560 |
| | $^5D_4 \rightarrow {}^7F_4$ | 17182 | 582 |
| | $^5D_4 \rightarrow {}^7F_3$ | 16129 | 620 |
| Tb(Ka-pa)(acac) | $^5D_4 \rightarrow {}^7F_5$ | 18518 | 540 |
| | | 18298 | 546 |
| | | 18214 | 549 |
| | $^5D_4 \rightarrow {}^7F_4$ | 17241 | 580 |
| | | 17182 | 582 |
| | | 17035 | 587 |
| | | 16949 | 590 |
| | $^5D_4 \rightarrow {}^7F_3$ | 16155 | 619 |
| | | 16103 | 621 |

previously observed by Yan and Zhou for terbium complexes immobilized on silica matrix.

In order to study the effect of thermal heating on the luminescence of the Tb(Ka-pa) hybrid matrix, the solid was submitted to different thermal treatments; the temperatures of these treatments were fixed at 200, 300, and 400 °C on the basis of the thermal behavior of the sample discussed before. Figures 7 and 8 show the excitation and emission spectra, respectively, of the samples Tb(Ka-pa), Tb(Ka-pa)-200, Tb(Ka-pa)-300, and Tb(Ka-pa)-400, which results are summarized in Table 5. The LMCT band at 275 nm is present in the excitation spectra of all the Tb(Ka-pa) samples (Figure 7), irrespective of the treatment temperature. This is a proof of the enhanced thermal stability of the complex grafted on the kaolinite matrix and corroborates the initial thermal analysis results. The results observed in the spectra agree with the decomposition of the picolinic acid present in interlayer space with rising heat-treatment temperature, as the intensity of the band at 275 nm decreases and that of the band at 310 nm increases. Indeed, for the sample treated at 400 °C, the band with maximum at 310 nm is more intense compared with the band at 275 nm. The change in the intensities of these bands is attributed to the interaction between the $Tb^{3+}$ cations and the surface of kaolinite matrix following decomposition of picolinic acid. Indeed, the initial thermal analysis data had shown the decomposition of these organic molecules at temperatures higher than 300 °C. Table 5 lists the results from the luminescence study of Tb complexes grafted on kaolinite.

The emission spectra (Figure 8) also display the characteristic bands corresponding to the transition from the excited ($^5D_4$) to the fundamental state ($^7F_{5,\ 4\ \text{and}\ 3}$). The decrease in the relative intensity of the emission bands with increasing temperature indicates again that the decomposition of the organic ligands promotes interaction between terbium and the hydroxyl groups of kaolinite. The lower lifetime values achieved for treatments at 300 °C and above confirm the thermal analysis data; that is that the organic ligand covalently grafted on the clay decomposes at temperatures higher than 300 °C, giving rise to the interaction between the kaolinite surface groups and $Tb^{3+}$ ions.

## 4. CONCLUSIONS

Luminescent hybrid materials with high purity have been prepared by grafting of terbium picolinate complexes on an inorganic matrix by means of a simple methodology. The precursor was produced by intercalation of picolinic acid into kaolinite, thereby resulting in a hybrid material. The $Tb^{3+}$ ion and the secondary ligand (acac) were then incorporated into the hybrid material by stirring in an ethanolic solution. The infrared spectra confirmed coordination of the $Tb^{3+}$ ions to the organic moieties of the hybrid organic−inorganic matrix. The thermal curves demonstrated the improved thermal stability of lanthanide complexes covalently grafted on kaolinite, which were stable up to 300 °C. The excitation spectra presented a wide band in the 275 nm region, characteristic of metal-to-ligand charge-transfer, while the emission spectra displayed bands related to the electronic transitions from the excited state $^5D_4$ to the $^7F_J$ states ($J$ = 5, 4, and 3), typical of the $Tb^{3+}$ ion, with the 4→5 transition presenting high intensity. After incorporation of the secondary ligand (acac), the spectroscopic features of the hybrid matrix luminescence were enhanced, which gave rise to high lifetime values. These results confirm that $Tb^{3+}$ cations complexed with the ligands present on hybrid organic−inorganic are promising green luminophores. The methodology employed herein for the design of the luminescent hybrid material is simple and applicable to the preparation of highly luminescent compounds based on clay minerals with high thermal stability and promising photoluminescence properties.

## ■ ASSOCIATED CONTENT

**Supporting Information.** Structure of picolinic acid, DTG curves, UV−vis spectra of various solids, and photoluminescence decay curves for the Tb-containing solids. This material is available free of charge via the Internet at http://pubs.acs.org.

## ■ AUTHOR INFORMATION

### Corresponding Author

*E-mail: eh.defaria@gmail.com (E.H.dF.); pscalefi@unifran.br (P.S.C.).

## ■ ACKNOWLEDGMENT

This work has been developed in the frame of an interuniversity collaboration between Spain and Brazil. The Brazilian group thanks the financial support from FAPESP, CAPES, and CNPq and the photoluminescence measurements carried on Rare Earth Laboratory at the Chemistry Department of FFCLRP-USP. The Spanish group thanks the financial support from Spanish Ministry of Science and Innovation, MICINN, European Regional Development Fund, (ERDF; reference MAT2010-21177-C02), and Castilla-y-León Regional Government (reference SA009A11-2).

## ■ REFERENCES

(1) Martins, T. S.; Isolani, P. C. *Quim. Nova* **2005**, *28*−*1*, 111–117.
(2) Li, W.; Wang, X.; Song, X.; Li, L.; Liao, D.; Jiang, Z. *J. Mol. Struct.* **2008**, *885*, 1–6.
(3) Zolin, V. F. *J. Alloys Compd.* **2004**, *380*, 101–106.
(4) Sabbatini, N.; Guardigli, M.; Lehn., J. M. *Coord. Chem. Rev.* **1993**, *123*, 201–228.
(5) Godlewska, P.; Macalik, L.; Hanuza, J. *J. Alloys Compd.* **2008**, *451*, 236–239.
(6) Nassar, E. J.; Serra, O. A. *Quim. Nova* **2000**, *23*, 16–19.
(7) Yan, B.; Zhou, B. *J. Photochem. Photobiol., A: Chem.* **2008**, *195*, 314–322.
(8) Sarakha, L.; Forano, C.; Boutinaud, P. *Opt. Mater.* **2009**, *31*, 562–566.
(9) Wang, Y.; Li, H.; Gu, L.; Gan, Q.; Li, Y.; Calzaferri, G. *Microporous Mesoporous Mater.* **2009**, *121*, 1–6.
(10) de Faria, E. H.; Marçal, A. L.; Nassar, E. J.; Ciuffi, K. J.; Calefi, P. S. *Mater. Research* **2007**, *10*, 413–417.
(11) Carlos, L. D.; Ferreira, R. A. S.; Bermudez, V. Z.; Ribeiro, S. J. L. *Adv. Mater.* **2009**, *21*, 509–534.
(12) Binnemans, K. *Chem. Rev.* **2009**, *109*, 4283–4374.
(13) de Faria, E. H.; Lima, O. J.; Ciuffi, K. J.; Nassar, E. J.; Vicente, M. A.; Trujillano, R.; Calefi, P. S. *J. Colloid Interface Sci.* **2009**, *335*, 210–215.
(14) Bizaia, N.; de Faria, E. H.; Ricci, G. P.; Calefi, P. S.; Nassar, E. J.; Castro, K. A. D. F.; Nakagaki, S.; Ciuffi, K. J.; Trujillano, R.; Vicente, M. A.; Gil, A.; Korili, S. *Appl. Mater. Interface* **2009**, *1*, 2667–2678.
(15) de Faria, E. H.; Ciuffi, K. J.; Nassar, E. J.; Vicente, M. A.; Trujillano, R.; Calefi, P. S. *Appl. Clay Sci.* **2010**, *48*, 516–521.
(16) Ávila, L. R.; de Faria, E. H.; Ciuffi, K. J.; Nassar, E. J.; Vicente, M. A.; Trujillano, R.; Calefi, P. S. *J. Colloid Interface Sci.* **2010**, *341*, 186–193.
(17) Tronto, J.; Ribeiro, S. J. L.; Valim, J. B.; Gonçalves, R. R. *Mater. Chem. Phys.* **2008**, *113*, 71–77.
(18) Wan, C.; Li, M.; Bai, X.; Zhang, Y. *J. Phys. Chem. C* **2009**, *113*, 16238–16246.
(19) Lezhnina, M.; Benavente, E.; Bentlage, M.; Echevarría, Y.; Klumpp, E.; Kynast., U. *Chem. Mater.* **2007**, *19*, 1098–1102.
(20) Sanchez, A.; Echeverría, Y.; Torres, C. M. S.; González, G.; Benavente, E. *Mater. Res. Bull.* **2006**, *41*, 1185–1191.
(21) Celedon, S.; Quiroz, C.; Gonzalez, G.; Torres, C. M. S.; Benavente, E. *Mater. Res. Bull.* **2009**, *4*, 1191–1194.
(22) Tunney, J. J.; Detellier, C. *Chem. Mater.* **1993**, *5*, 747–748.
(23) Brandt, K. B.; Elbokl, T. A.; Detellier, C. *J. Mater. Chem.* **2003**, *13*, 2566–2572.
(24) Letaief, S.; Tonle, I. K.; Diaco, T.; Detellier, C. *Appl. Clay Sci.* **2008**, *42*, 95–101.
(25) Itagaki, T.; Kuroda., K. *J. Mater. Chem.* **2003**, *13*, 1064–1068.
(26) Tunney, J. J.; Detellier, C. *Clays Clay Miner.* **1994**, *42*, 552–560.
(27) Letaief, S.; Detellier, C. *J. Mater. Chem.* **2005**, *15*, 4734–4740.
(28) Frost, R. L.; Kristof, J.; Paroz., G. N.; Kloprogge, J. T. *J. Phys. Chem. B* **1998**, *102*, 8519–8532.
(29) Letaief, S.; Detellier, C. *Chem. Commun.* **2007**, 2613–2615.
(30) Bünzli, J. G.; Piguet, C. *Chem. Soc. Rev.* **2005**, *34*, 1048–1077.
(31) Escribano, P.; Júlian-Lopez, B.; Planelles-Aragó, J.; Cordoncillo, E.; Viana, B.; Sanchez, C. *J. Mater. Chem.* **2008**, *18*, 23–40.
(32) Franville, A. C.; Zambon, D.; Mahiou, R.; Chou, S.; Troin, Y.; Cousseins, J. C. *J. Alloys Comp.* **1998**, *275*, 831–834.
(33) Zolin, V. F.; Tsaryuk, V. I.; Kudryashova, V. A.; Zhuravlev, K. P.; Gawryszewska, P.; Szotstak, J. *J. Alloys Comp.* **2008**, *451*, 149–152.
(34) Lis, S.; Hnatejko, Z.; Barczynski, P.; Elbanowski, M. *J. Alloys Comp.* **2002**, *344*, 70–74.
(35) Calefi, P. S.; Ribeiro, A. O.; Pires, A. M.; Serra., O. A. *J Alloys Comp.* **2002**, *344*, 285–288.
(36) Marczenko, Z. *Separation and Spectrophotometric Determination of Elements*; John Willey & Sons Eds.: London, 1986, 468.
(37) Joussein, E.; Petit, S.; Churchman, J.; Theng, B.; Righ, D.; Delvaux, B. *Clay Miner.* **2005**, *40*, 383–426.
(38) Nakagaki, S.; Wypych, F. *J. Colloid Interface Sci.* **2007**, *315*, 142–57.
(39) Gardolinski, J. E. F. C.; Lagaly, G. *Clay Miner.* **2005**, *40*, 547–556.
(40) Valášková, M.; Rieder, M.; Matějka, V.; Čapková, P.; Slíva., A. *Appl. Clay Sci.* **2007**, *35*, 108–118.
(41) Lima, P. P.; Malta, O. L.; Alves Junior, S. *Quim. Nova* **2005**, *28*, 805–808.
(42) Reinhard, C.; Güdel, H. U. *Inorg. Chem.* **2002**, *41*, 1048–1055.
(43) Supkowski, R. M.; Horrocks, DeW. W., Jr. *Inorg. Chim. Acta* **2002**, *340*, 44–48.
(44) Yan, B.; Zhou, B. *J. Photochem. Photobiol., A: Chem.* **2008**, *195*, 314–322.